

# Buried Utility Pipeline Mapping based on Street Survey and Ground Penetrating Radar

Huanhuan Chen<sup>1</sup> and Anthony G Cohn<sup>2</sup>

## 1 INTRODUCTION

In the UK and many other countries, underground networks are used to deliver a range of services to households and industries. Maintaining and upgrading these networks are major undertakings. In order to avoid unnecessary holes dug in wrong places, prior to invasive works it is normally required that excavators should request and obtain record information from all relevant utilities to identify what is buried where. However, the mapping information supplied by utility companies is often of limited use as asset records are usually inaccurate and incomplete. Thus a street survey is often conducted using sensor devices, such as ground penetrating radar (GPR). However, these are costly, and forming a complete picture combining the expectation of the map and the sensor data is an expert task. This paper will investigate an algorithm for utility pipeline mapping based on street survey and GPR data.

## 2 UTILITY PIPELINE MAPPING ALGORITHM

GPR has been widely used in the detection and mapping of subsurface utilities. However, it is difficult to estimate the pipe direction based on the GPR scans, which is very important for utility mapping. To solve this problem, this paper proposes to use a set of scans at each scan location to estimate the direction of the buried pipes.

Fig 1(a) shows the situation when the GPR operates perpendicularly to the pipe. Buried pipes typically generate a hyperbola [1, 2] in a GPR scan. In this case, the hyperbolae in each GPR scan are exactly the same. The real-world GPR image is shown in Fig 1(d).

If the scan direction is parallel to the direction of the pipe, there is one hyperbola (small pipe) or one linear line (large pipe) in only one GPR scan or there are incomplete hyperbolae in one or two GPR scans, which is illustrated in Figs 1(b) and 1(e).

The most common situation is that GPR scans the pipe at an angle. As illustrated in Figs 1(c) and 1(f), there should be one hyperbola in each GPR scan for each pipe. However, the  $x$  position of each hyperbola is different as the  $x$  axis records the distance from the starting point to the point where GPR detects the pipe. The angle can be estimated by  $\alpha = \arctan x/d$ , where  $x$  is the distance between the first and last scan,  $d$  is the horizontal distance between starting points of the first scan and the last scan. In practical work, the distance  $d$  is fixed and each scan is 3 metres in our data, i.e. the range of the  $x$  axis is 3 metres and each increment in  $x$  direction represents 5cm. To facilitate this model, this paper employs our recently proposed algorithm to determine the position of hyperbolae automatically based

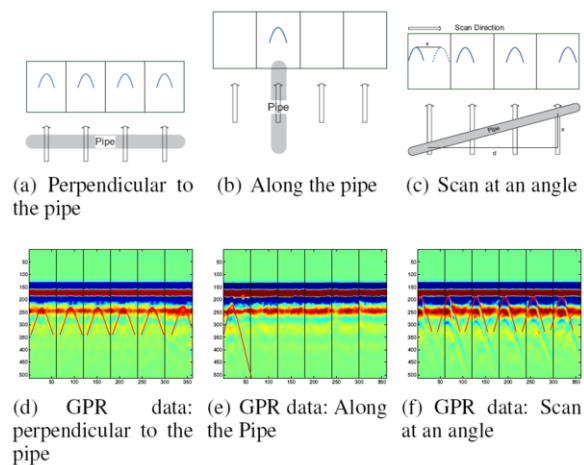


**Figure 1.** The model to estimate pipe direction by GPR data and the corresponding GPR data illustration with hyperbola identification.

on orthogonal distance fitting and classification expectation maximization algorithm [1, 2]. In the following, we will incorporate street survey data, such as manhole locations and the possible direction of these pipes, with GPR scans for utility mapping. Two kinds of inputs are presented in this algorithm.

- Data from manhole investigation. The data consists of a series of manhole locations and the pipe directions  $(x_{i,k}, y_{i,k}, \theta_{i,k})_{i=1}^m$ , where  $m$  is the number of manholes in the data,  $k$  is the number of pipes through manhole  $i$  and  $\theta_{i,k}$  is the direction of the pipe  $k$  through manhole  $i$ . The covariance matrix  $C_{i,k}$  for each triplet  $(x_{i,k}, y_{i,k}, \theta_{i,k})$  is provided for uncertainty consideration.
- GPR scanning locations and the estimated pipe directions  $(x_{g,k}, y_{g,k}, \theta_{g,k})_{g=1}^n$ , where  $k$  is the pipe coming through  $(x_g, y_g)$ . The uncertainty is represented by  $C_{g,k}$  in the GPR analysis; note that the uncertainty  $C_{g,k}$  is larger than  $C_{i,k}$  as manhole investigation is relatively more reliable than GPR scans.

The utility map is created by data association algorithms, which connect the observed manholes and GPR detections. In this paper, nearest neighbour (NN) standard filter and joint compatibility branch and bound (JCBB) methods are employed.

The NN standard filter simply takes the nearest validated measurement to connect the map. A pipe will be regressed from the starting point to the possible ending point. The uncertainty of the starting point will be regressed to the ending point area. As we see from Fig 2(a), the final uncertainty consists of location uncertainty and the

<sup>1</sup> University of Leeds, UK, email: H.H.Chen@leeds.ac.uk

<sup>2</sup> University of Leeds, UK, email: A.G.Cohn@leeds.ac.uk

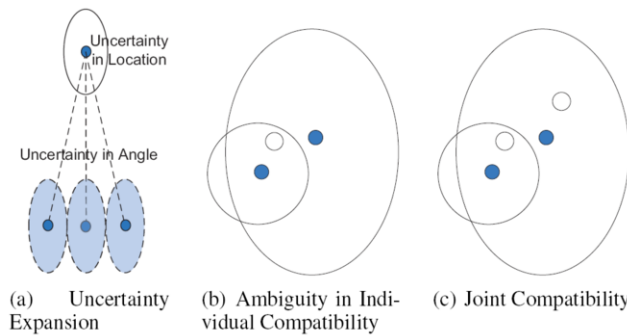


**Figure 2.** Illustration of Individual Compatibility and Joint Compatibility in Map Connection. The blue (gray) points represent the ending manholes and the circle (blank) points represent the regressed starting points.

angle uncertainty. The two points are connected only when the Mahalanobis distance of two survey points (either manhole or GPR with pipe direction) is smaller than a threshold, 0.99 in this paper.

The NN algorithm uses individually compatible pairings to connect points to form the maps. However, individually compatible pairings are not guaranteed to be jointly compatible to form a consistent hypothesis. Even if street observations and GPR analysis results are independent, correlations in the uncertainty of manhole locations might be presented. The problem can be illustrated in Fig 2(b). The blank circular point is within the neighbourhood area of both blue points. In this case, it is difficult to judge which one to connect to.

To solve this problem, JCBB is proposed to measure the joint compatibility of a set of pairings, and is known to be more robust in complex environments. The mechanics of JCBB are illustrated in Fig 2(c), where there are two corresponding points and two ending points, and the error of these two pairings are correlated. JCBB is preferable to NN in the situation that the starting manhole/GPR observations uncertainty are correlated, which often exists as the pipes through nearby manholes often follow the roughly similar directions and thus the uncertainties of these estimations are not independent.

### 3 EXPERIMENTAL STUDY

Two real-world data sets have been employed. Each data set consists of an AutoCAD drawing, sets of GPR point scans and the street survey results. Each GPR point scan consists of six pushes in a three metres neighbourhood area. Therefore,  $d$  equals to three metres in these experiments. Figs 3(a) and 3(d) show the bird's eye views of the survey sites, which are from the Birmingham area, UK. We only consider utilities with manholes in the survey area. Figs 3(b) and 3(e) provide the AutoCAD drawings of the survey sites with GPR scan boxes (small box with a line going through the box), the scans start from the line and go forward 3m perpendicular to the line, in the direction of the box side of the line. The Autocad drawing also show the estimated underground asset location as given by the survey company. These are used in lieu of ground truth to compute the error rate (Table 1). Besides these data, there is a data file for each survey showing the location of each manhole and the possible directions of the pipes through these manholes.

In these experiments, the uncertainty for the manhole location and GPR point scan are chosen as 0.2 and 0.4 metre, respectively. The uncertainty of pipe directions is fixed to 8 and 15 degrees for manhole observation and GPR scans, respectively. We illustrate the obtained

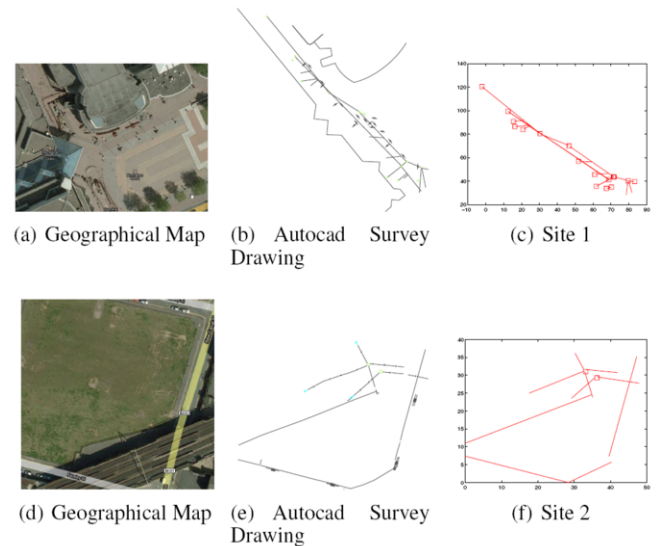


**Figure 3.** Geographical Map, Autocad Survey Drawing and the obtained Utility Mapping

map using JCBB in Figs 3(c) and 3(f) and the detailed comparisons between nearest neighbour (NN) method and JCBB are presented in Table 1.

According to the table, NN makes 8 and 2 connection errors in the first and second data sets respectively while JCBB makes 3 and 0 connection errors in the first and second data set. The computational time of JCBB is larger than that of NN.

The algorithm presented here represents an initial prototype to fuse the sensor output of a multi-sensor device being researched and constructed to improve buried asset location detection [3]. Ultimately, this project aims at facilitating the reliable detection and mapping of *all* buried assets for greatly improved street-working.

**Table 1.** The comparisons between NN and JCBB. The computational environment is Linux with Intel 4 core 2.5G CPU and 4G RAM.

Experiments	Algorithm	Error #	Computational Time
Site 1	NN	8	0.0573s
Site 1	JCBB	3	4.3s
Site 2	NN	2	0.0461s
Site 2	JCBB	0	2.1s

### ACKNOWLEDGEMENTS

This research is supported by an EPSRC grant (EP/F06585X/1).

### REFERENCES

- [1] H. Chen and A. G. Cohn, 'Probabilistic conic mixture model and its applications to mining spatial ground penetrating radar data', in *Workshops in SIAM Conference on Data Mining (SDM10)*, (2010).
- [2] H. Chen and A. G. Cohn, 'Probabilistic robust hyperbola mixture model for interpreting ground penetrating radar data', in *IEEE World Congress on Computational Intelligence (WCCI'10)*, (2010).
- [3] A. Royal, C. Rogers, P. Atkins, M. Brennan, D. Chapman, A. Cohn, P. Lewin, N. Metje, J. Muggleton, S. Pennock, et al., 'Briefing: stakeholder perspectives of buried utility mapping', *Proceedings of the ICE-Municipal Engineer*, **163**(1), 3–7.